Characterization of Superconducting Single Photon Detectors fabricated on MgO substrates

R. Leoni, A. Gaggero, F. Mattioli, and M.G. Castellano

Istituto di Fotonica e Nanotecnologie, CNR, Via Cineto Romano 42, 00156 Roma, Italy.

P. Carelli

Università dell'Aquila, Monteluco di Roio, 67040 L'Aquila, Italy.

F. Marsili, D. Bitauld, M. Benkahoul, F. Lévy and A. Fiore

Ecole Polytechnique Fédérale de Lausanne, Station 3, CH-1015 Lausanne, Switzerland.
Corresponding author: roberto.leoni@ifn.cnr.it

Electrical and optical characterization has been performed on several superconducting single photon detectors (SSPDs) consisting of meanders made of ultrathin NbN films. The NbN films, with thickness ranging from 150nm to 3nm, were deposited by dc magnetron sputtering on MgO substrates kept at temperature T=400°C. This deposition process carried out at low temperature opens the way of monolithic integration with other photonic devices. The superconducting properties of NbN films and the critical design parameters that affect the quantum efficiency (QE) have been optimized. In particular, by measuring the switching current distribution of each stripe of the meander the process uniformity has been studied. Optical measurements on the fabricated SSPDs showed a QE ≈20% at 4.2 K for photons with a wavelength of 1300 nm.
PACS numbers: 85.25.Pb, 81.16.Nd

Received 22 July 2007 ; Accepted 15 September 2007

1. INTRODUCTION

Several applications such as high-bandwidth interplanetary communications[1], quantum key distribution[2] and test of highspeed

semiconductor circuits[3] need high counting-rate detectors capable of sensing single photons in the near infrared region. Recently, a fast nanoscale photonic device based on a ultrathin (about 3÷5 nm) superconducting material patterned in meander shape geometry, the superconducting single photon detector (SSPD)[4] has shown extremely promising results.

The SSPDs sensing mechanism is based on the combination of the submicrometric width of a stripe (about 100 nm) and the transport properties of the superconducting film[5]. Due to the biasing point and the low impedance of the electromagnetic environment in which the device is embedded, as soon as a single photon is adsorbed in the stripe, in a time of the order of 10 ps a normal "hot spot" (20 nm size for 850 nm photon) is created and successively a voltage pulse is generated when the whole section of the film becomes normal[6].

Integration of SSPDs with advanced optical structures such as waveguides, microcavities and read-out electronics, could be very useful for all the application mentioned above. Up to now, NbN films used for SSPDs have been grown on sapphire substrates at high temperatures (about 900°*C*)[7] limiting this kind of integration. Here we show that NbN SSPDs can be implemented also on MgO substrates and at lower deposition temperatures (about 400°*C*), compatible with monolithic integration.

A meander geometry is used to enhance the filling factor of the detection area and hence the detection efficiency of the device. SSPDs were fabricated on high quality NbN films of different thicknesses deposited under optimal conditions. The geometric parameters were optimized to obtain higher quantum efficiencies. In particular, we have measured the critical current distributions of each stripe of a test meander structure in order to directly probe the linewidth homogeneity resulting from our fabrication process.

2. DEVICE FABRICATION

Current controlled dc magnetron sputtering has been used to grow NbN films ranging from 150 nm to 3 nm in thickness on epitaxial-quality single crystal MgO <100> substrates. Our setup allowed us to use power densities of the order of 10 W/cm^2, high enough to grow high quality NbN films on a substrate at temperature as low as T_S = 400°C. The superconducting properties of NbN films, T_C, ΔT_C and Residual Resistivity Ratio (RRR, the ratio between the resistivity at 300 K and at 20 K) were optimized studying both the effects of the pressure P_{tot} in the deposition chamber and the composition of the reactive gases (Ar and N_2) on film properties[8]: P_{tot}=2.5 mTorr, P_{N2}/P_{tot} = 33%, were found to be the optimal deposition parameters, resulting in a T_C=16.1 K, with a ΔT_C =60 mK and a

RRR = 1 for a 150 nm thick film. Decreasing the thickness of films led to a slight degradation of their superconducting properties but even a 3nm thick film has a T_C =8.6 K, with ΔT_C =900 mK and RRR=0.6.

The nanolithography steps have been carried out by using an electron beam lithography (EBL) system equipped with a field emission gun with electrons accelerated at high voltage (100 kV). A two step process is needed to obtain the whole device[9,10]. In the first step pads and markers (Ti/Au 70 nm thick) are fabricated by using lift off technique via a PMMA stencil mask, (PMMA stays for Polymethyl Methacrylate, positive tone electronic resist). In the second step, an HSQ mask (HSQ stays for hydrogen silsesquioxane, negative tone resist) properly aligned to the previous layer by using the markers above mentioned, is defined on top of the sample and it is used to etch the NbN film. All the unwanted material, i.e. the material not covered by the HSQ mask and the Ti/Au film, is removed by using a fluorine based reactive ion etching (RIE).

3. EXPERIMENTAL RESULTS

In order to study the linewidth uniformity and to set the critical parameters of the fabrication process, it is more convenient to study the variations of the critical current along the meander instead of the corresponding resistance changes, because a small constriction in the width can affect considerably the critical current of a stripe without changing too much its normal resistance. Several SSPDs, on purpose designed to allow the electrical access to each stripe of the meander, have been used to study the "local" distribution of the critical currents (see figure 1 a). The thicknes of the NbN films used for those devices was 10 nm.

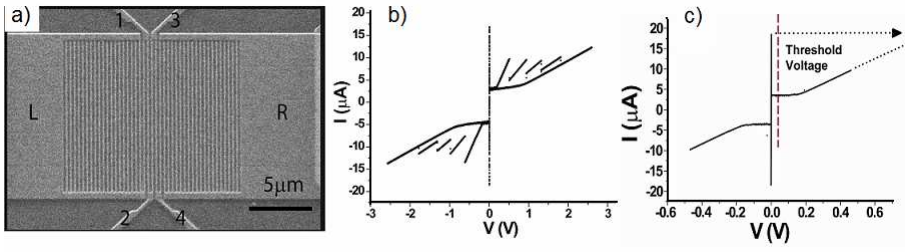

Fig. 1: a) Scanning electron micrograph of a SSPD made of five stripes, 100 nm wide, 10 nm thick, 150 nm spacing. Each stripe was accessed by separate electrical connections (labelled L, 1, 2, 3, 4, R). Lateral dummy stripes are used to improve linewidth uniformity. b) I-V curve of the SSPD shown in a) as recorded by using pads L and R. c) I-V characteristics of a single stripe of the meander shown in a) as recorded by using pads 1 and 2. The threshold

value for the comparator is also shown. The I-V characteristics are measured at 4.2K.

Figure 1b) shows the I-V characteristics of a SSPD with large filling factor (about 40%). The transitions from superconducting to normal state of each single stripe are clearly visible in correspondence of the abrupt change of the circulating current. It should be noted that the amplitudes of these switching currents change from stripe to stripe, with the larger one corresponding to the first switch. This is apparently in contradiction with the consideration that the first transition must correspond to the stripe with lower critical current. Differently, in case of SSPDs with low filling factor (about 6%) the amplitudes of the switching currents are almost the same for each stripe. Thermal effects are responsible for this behaviour. The joule dissipation of the part of the meander already in the normal state increases the local temperature and decreases the critical current of the other superconducting stripes, effect that is relevant in the case of large filling factors. We have also measured the critical current of individual stripes by recording their I-V curves (figure 1c), but this measurement is quite inaccurate as it is well know the amplitude is statistically distributed because of thermal fluctuations. Instead, we have developed a more accurate measurement of the uniformity of the critical current by measuring the switching current distributions. We point out that the observed thermal effects are not important when the meander is operated as single photon detector since it is biased below its critical current I_c, where the whole device is in the superconducting state.

To measure the switching current distributions of a single stripe the meander was current biased and the voltage across a single stripe was sent to a voltage comparator. The voltage threshold value of the comparator (dashed line in figure 1c), is set very close to the superconducting branch: in this way as soon as the transition takes place and the voltage starts to increase, a comparator sends a TTL (Transistor-Transistor Logic) pulse toward the acquisition board that acquires the current that is circulating in the nanostripe at that time. Repeating several times this process, a plot of the number of these switching events as a function of the current is obtained for each stripe of the meander (switching distributions). Figure 2 a) shows the results for the meander of figure 1. The critical current non uniformity is about 6% for this meander with filling factor 40%, indicating that the fabrication process has achieved a good control of the linewidth homogeneity confirmed also by high resolution SEM imaging on the meanders.

On the basis of these encouraging results we proceeded also with the SSPD optical characterization performed on 5x5 μm^2 area SSPDs (21

stripes, without individual electrical access) with filling factors ranging from 40% to 60% and linewidth from 60 nm to 100 nm. The meanders were contacted through pads patterned as a 50 Ω coplanar transmission line. We selected the devices with the highest critical current because these are the best candidate to obtain high QE.

The photons were fed to the SSPDs through a single-mode optical fiber. The attenuation of the whole system was about 10^{-7}, and the average number of incident photons per optical pulse was around 0.5. As expected for a true single photon detection regime, the dependence of the number of detector counts per second on the average number of photons per pulse was found to be linear for the photon fluxes used in QE measurements[11]. The QE at bias current I_B was calculated as: $QE = (N_c - DK)/N_{ph}$, where N_c is the number of detection events registered by the counter in one second, N_{ph} is the number of photons incident on the device area in the same time and DK is the dark counts rate at I_B determined as the number of counts registered in one second when the SSPD optical input was blocked.

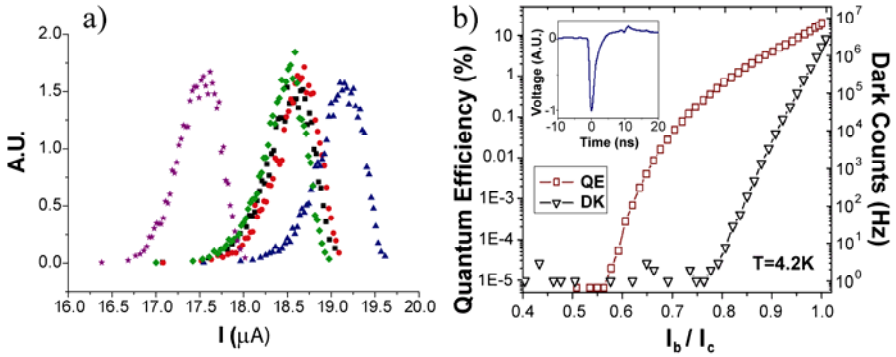

Fig. 2 (Color on-line): a) Current switching distributions of the five stripes of the SSPD shown in figure 1, measured at 4.2 K. b) Quantum efficiency (QE) and dark counts (DK) as a function of the normalized bias current I_B/I_c at 4.2 K for the SSPD in the single photon detection regime. The SSPD is 5x5 μm^2 in area, 100 nm linewidth, 40% filling factor and 4 nm NbN in thickness. The incident photon wavelength was 1.3 μm. The inset shows a time resolved response pulse.

At 4.2 K the best performance was obtained with a SSPD with 100 nm linewidth, filling factor 40% and 4 nm thickness, which reaches QE=20% for 1.3 μm wavelength photons (figure 2b) which is a state of the art value at the temperature of the experiment even if a higher QE and a much lower DK can be obtained by cooling the device down to 2 K. The time resolved

response pulse of our best SSPD showed a full width at half maximum (FWHM) of 1.6 ns (inset figure 2b).

We thank S. Pagano for discussions and H. Jotterand for technical support. The work was supported through the research project SINPHONIA by the European Commission under contract number NMP4-CT-2005-16433, and by the Swiss National Science Foundation.

REFERENCES

1. D. M. Boroson, R.S. Bondurant, and J.J. Scozzafava, Proc. SPIE **5338**, 37 (2004).
2. N. Gisin, G. Ribordy, W. Tittel, and H. Zbinden, Rev. Mod. Phys. **74**, 145 (2002).
3. S. Somani, S. Kasapi, K. Wilsher, W. Lo, S. Roman, and G. Gol'tsman, J. Vac. Sci. Technol. B **19**, 2766 (2001).
4. G.N. Gol'tsman, O. Okunev, G. Chulkova, A. Lipatov, A. Semenov, K. Smirnov, B. Voronov, A. Dzardanov, C. Williams, and R. Sobolewski, Appl. Phys. Lett. **79**, 705 (2001).
5. A. Semenov, G. Gol'tsman, and A. Korneev, Physica C **351**, 349 (2001).
6. K.S. Il'in, I.I. Milostnaya, A.A. Verevkin, G.N. Gol'tsman, E.M. Gershenzon, and R. Sobolewski, Appl. Phys. Lett. **73**, 3938 (1998).
7. G. Gol'tsman, O. Okunev, G. Chulkova, A. Lipatov, A. Dzardanov, K. Smirnov, A. Semenov, B. Voronov, C. Williams, and R. Sobolewski, IEEE Trans. Appl. Supercond. **11**, 574 (2001).
8. J.C. Villegier, L. Vieux-Rochaz, M. Goniche, P. Renard, and M. Vabre, IEEE Trans. Mag. **21**, 498 (1984).
9. R. Leoni, F. Mattioli, M.G. Castellano, S. Cibella, P. Carelli, S. Pagano, D. Perez de Lara, M. Ejrnaes, M.P. Lisitskyi, E. Esposito, R. Cristiano, and C. Nappi, Nucl. Instrum. Methods Phys. Res. A **559**, 564 (2006).
10. F. Mattioli, R. Leoni, A. Gaggero, M.G. Castellano, P. Carelli, F. Marsili, and A. Fiore, J. Appl. Phys. **101**, 054302 (2007).
11. A. Verevkin, J. Zhang, R. Sobolewski, A. Lipatov, O. Okunev, G. Chulkova, A. Korneev, K. Smirnov, G.N. Gol'tsman, and A. Semenov, Appl. Phys. Lett. **80**, 4687 (2002).